THE JOURNAL OF PHYSICAL CHEMISTRY Letters

Letter

pubs.acs.org/JPCL

Concerted HO_2 Elimination from α-Aminoalkylperoxyl Free Radicals: Experimental and Theoretical Evidence from the Gas-Phase $NH_2{}^{\bullet}CHCO_2{}^- + O_2$ Reaction

Gabriel da Silva,*[,†] Benjamin B. Kirk,[‡] Celli Lloyd,[‡] Adam J. Trevitt,[‡] and Stephen J. Blanksby*[,‡]

[†]Department of Chemical and Biomolecular Engineering, The University of Melbourne, Victoria 3010, Australia

[‡]ARC Centre of Excellence for Free Radical Chemistry and Biotechnology, School of Chemistry, University of Wollongong, NSW 2522, Australia

Supporting Information

ABSTRACT: We have investigated the gas-phase reaction of the α-aminoacetate (glycyl) radical anion ($NH_2{}^{\bullet}CHCO_2{}^-$) with O_2 using ion trap mass spectrometry, quantum chemistry, and statistical reaction rate theory. This radical is found to undergo a remarkably rapid reaction with O_2 to form the hydroperoxyl radical ($HO_2{}^{\bullet}$) and an even-electron imine ($NHCHCO_2{}^-$), with experiments and master equation simulations revealing that reaction proceeds at the ion−molecule collision rate. This reaction is facilitated by a low-energy concerted $HO_2{}^{\bullet}$ elimination mechanism in the $NH_2CH(OO{}^{\bullet})CO_2{}^-$ peroxyl radical. These findings can explain the widely observed free-radical-mediated oxidation of simple amino acids to amides plus α-keto acids (their imine hydrolysis products). This work also suggests that imines will be the main intermediates in the atmospheric oxidation of primary and secondary amines, including amine carbon capture solvents such as 2-aminoethanol (commonly known as monoethanolamine, or MEA), in a process that avoids the ozone-promoting conversion of $^{\bullet}NO$ to $^{\bullet}NO_2$ commonly encountered in peroxyl radical chemistry.

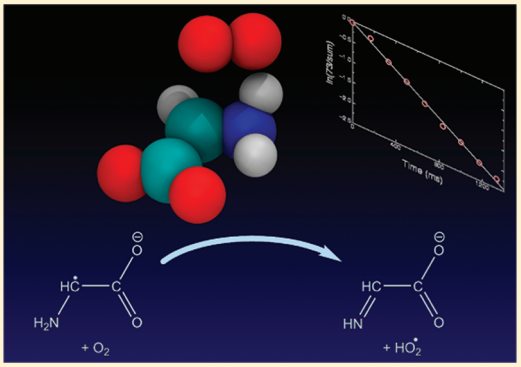

SECTION: Kinetics, Spectroscopy

Peroxyl radicals are key intermediates in the free radical oxidation of biomolecules,[1] the photochemical degradation of organic compounds in the atmosphere,[2] and the combustion of hydrocarbon fuels.[3] Accordingly, the chemistry of peroxyl radicals formed from O_2 addition to carbon-centered hydrocarbon radicals has been extensively investigated. There has been relatively little work, however, on the oxidation of a ubiquitous class of carbon-centered radicals, those substituted with amine functional groups. These aminoalkyl radicals are formed in vivo via ionizing radiation and free radical attack of amino acids.[4] Oxidative damage of biomolecules constructed from amino acids has been implicated in a raft of human diseases and conditions. In combustion, aminoalkyl radicals are unavoidable intermediates in the catalytic $DeNO_x$ process. Here, the $^{\bullet}NH_2$ radical is intentionally generated so that it can convert $^{\bullet}NO$ to harmless N_2 and H_2O, although $^{\bullet}NH_2$ will also associate with alkyl radicals to yield alkylamines.[5,6] Finally, amines are released to the atmosphere through a variety of anthropogenic and biogenic activities,[7] where they react with $^{\bullet}OH$ to form aminoalkyl radicals that can subsequently associate with O_2. Amine solvents, such as monoethanolamine (MEA), are the benchmark technology proposed for carbon capture and sequestration (CCS) from coal-fired power plants to mitigate CO_2 emissions,[8] and large new emission sources of these volatile amines to the atmosphere are expected, with little understanding of the impact that this will have on the quality of urban air.[9]

Of the various intermediates that can form in the free-radical-initiated oxidation of amines, α-aminoalkyl radicals ($R^{\bullet}CHNH_2$) are of particular interest. These radicals can be readily produced from primary amines due to weakening of the alpha C−H bonds that can be attributed to radical stabilization arising from hyperconjugation of the radical site with the dative nitrogen lone pair *and* the C−N sigma bonding orbital. Here, we present a combined experimental and theoretical study of the oxidation of these α-aminoalkyl radicals. By synthesizing a charge-tagged analogue, we have performed the first definitive product detection study of an α-aminoalkyl radical + O_2 reaction. There is a large body of literature on the use of tailored radical ions as proxies for neutral systems,[10,11] and when coupled with theory, this allows us to extrapolate results from the anionic system to important neutral analogues.

We have synthesized the α-aminoacetate radical anion $NH_2{}^{\bullet}CHCO_2{}^-$ in an ion trap mass spectrometer and observed the products and kinetics of its reaction with dioxygen. Experimental results are compared to theoretical kinetic

Received: January 31, 2012
Accepted: February 29, 2012
Published: February 29, 2012

Scheme 1. Gas-Phase Synthesis of the α-Aminoacetate Radical Anion from ESI of Glutamic Acid to Form the Glutamate Dianion with Subsequent PD, Yielding Spontaneous Decarboxylation and Elimination of Ethylene by CID

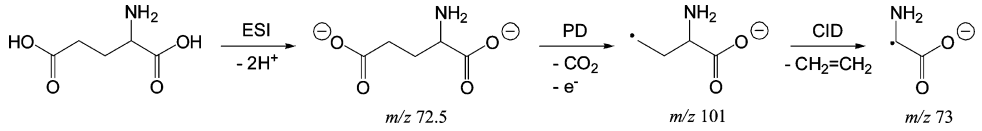

simulations (master equation/RRKM theory) based on an ab initio energy surface. Further comparison is made between the theoretical energy surface for α-aminoacetate oxidation and that of the prototypical aminomethyl radical $NH_2CH_2^{\bullet}$. A novel mechanism is revealed for the dissociation of α-aminoalkylperoxyl radicals that involves concerted $HO_2^{\bullet}$ radical elimination, and this process is expected to impact amine oxidation in the human body, in Earth's atmosphere, and in flames. In addition, the $NH_2^{\bullet}CHCO_2^-$ radical anion studied here is the archetypal amino acid radical anion. Indeed, this glycyl radical anion is a major product of the reaction of deprotonated glycine with hydroxyl radical[12,13] and has also been invoked as an intermediate in enzyme-driven formation of *p*-cresol from deprotonated tyrosine.[14] As a result, there have been numerous studies of the glycyl radical anion in solution,[15,16] but to our knowledge, this study provides the first evidence for the isolation of this important intermediate.

The α-aminoacetate radical anion was synthesized in the gas-phase according to the sequence depicted in Scheme 1, and the mass spectra resulting from isolation of this species in the presence of dioxygen are provided in Figure 1. In these

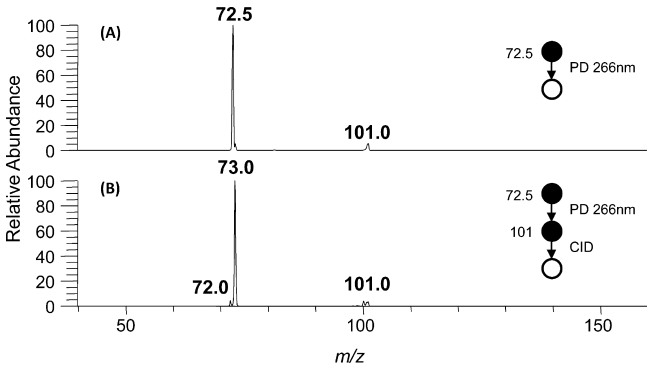

Figure 1. Gas-phase synthesis of the α-aminoacetate radical anion ($NH_2^{\bullet}CHCO_2^-$). (A) 266 nm PD of the glutamate dianion at *m/z* 72.5 produces the decarboxylation products at *m/z* 101. (B) CID of the *m/z* 101 ion population leads to $NH_2^{\bullet}CHCO_2^-$ radical ion formation (*m/z* 73) via the expulsion of C_2H_4 (cf. Scheme 1).

experiments, a methanolic solution of glutamic acid was subjected to electrospray ionization (ESI) to yield the glutamate dianion at *m/z* 72.5 (i.e., 145/2) in an ion trap mass spectrometer. Mass selection of the dianion and subsequent photodissociation (PD) at 266 nm achieved electron detachment and concomitant elimination of CO_2 to form a radical ion population at *m/z* 101. Isotope labeling allowed for differentiation of the two carboxylate moieties and revealed that no ionic products were derived from loss of the backbone carboxylate (see Supporting Information), and thus *m/z* 101 can be unambiguously assigned to $^{\bullet}CH_2CH_2CH(NH_2)CO_2^-$, as indicated in Scheme 1. This intermediate radical anion was mass-selected with subsequent collision-induced dissociation (CID) driving the loss of C_2H_4 and generating the target $NH_2^{\bullet}CHCO_2^-$ radical anion at *m/z* 73.

Following gas-phase synthesis and isolation of the α-aminoacetate radical anion, it was allowed to undergo reaction with background O_2 in the ion trap for times ranging from 30 ms to 1 s. The resultant mass spectra are depicted in Figure 2.

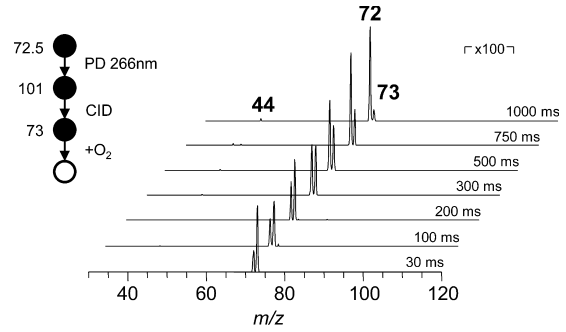

Figure 2. Relative ion abundances versus time for the α-aminoacetate radical anion ($NH_2^{\bullet}CHCO_2^-$) + O_2 reaction. The $NH_2^{\bullet}CHCO_2^-$ ion (*m/z* 73) was synthesized as shown in Figure 1 and held in the ion trap for up to 1 s to react with adventitious O_2. The only significant reaction products correspond to $+O_2 - HO_2^{\bullet}$ (*m/z* 72) and $+O_2 - [HO^{\bullet} + CO_2]$ (*m/z* 44).

Notably, these spectra show an absence of product ions at *m/z* 105 (even with a 100-fold magnification of the signal) that would correspond to detection of an intermediate peroxyl radical; rather, the major product ion is at *m/z* 72, with a minor product also detected at *m/z* 44. The major product corresponds to loss of 1 Da from the parent (i.e., $+O_2 - HO_2^{\bullet}$), whereas the minor product ion indicates loss of 29 Da (i.e., $+O_2 - [HO^{\bullet} + CO_2]$). Decay of the *m/z* 73 ion demonstrates first-order behavior in a natural log plot of ion intensity versus time, with a corresponding pseudo-first-order rate constant of 1.7 ± 0.1 s^{-1} (see Supporting Information). Using an O_2 concentration of 2.65 × 10^9 molecule cm^{-3} (confirmed by a calibration reaction),[17] this yields a total second-order rate coefficient of 6.4 (±0.3) × 10^{-10} cm^3 $molecule^{-1}$ s^{-1}. Considering that the ion−molecule collision rate constant for α-aminoacetate + O_2 is 6.24 × 10^{-10} cm^3 $molecule^{-1}$ s^{-1}, our results indicate a remarkable reaction efficiency of 100% (within the statistical uncertainty of the measurement). As a consequence of the high reactivity of O_2 toward this radical, the *m/z* 73 ion could not be isolated in the presence of elevated O_2 concentrations (only *m/z* 72 was obtained). However, these experiments did demonstrate that increasing concentrations of O_2 resulted in concomitant depletion of *m/z* 73 and increased formation of the *m/z* 72 product, confirming the involvement of dioxygen in this reaction (see Figure S3, Supporting Information).

A theoretical energy surface for the α-aminoacetate + O_2 reaction is provided as Figure 3. The initial addition of dioxygen to the radical site is barrierless and exothermic by around 36 kcal mol^{-1}. In the gas phase, this provides the

dx.doi.org/10.1021/jz300118k | J. Phys. Chem. Lett. 2012, 3, 805−811

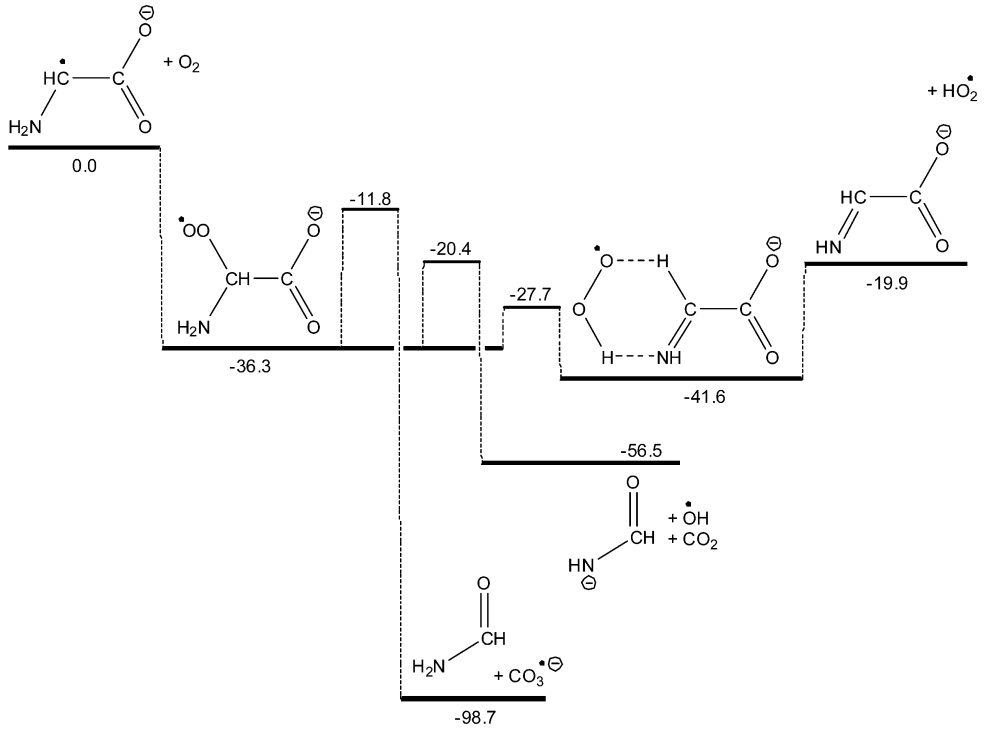

Figure 3. Ab initio energy surface for the α-aminoacetate radical anion ($NH_2{}^{\bullet}CHCO_2^-$) + O_2 reaction. G3SX enthalpies for 0 K are shown in units of kcal mol^{-1}.

peroxyl radical adduct with excess internal energy with which to surmount subsequent barriers to unimolecular transformation. The peroxyl radical can expel the carbonate radical anion, $CO_3{}^{\bullet-}$, in a reaction that is highly exothermic and proceeds at 11.8 kcal mol^{-1} below the entrance channel energy. The carbonate radical anion has been recently identified as the principal product of the $^{\bullet}CH_2CO_2^-$ + O_2 reaction[18] and is also observed for other carboxylate-substituted alkyl radicals.[19] Note that this reaction has been shown to proceed with a relatively high reaction efficiency under similar experimental conditions.[18] The absence of any m/z 60 signal in the α-amino-substituted form of this reaction (cf. Figure 2, where it is absent even at long reaction times) provides strong evidence that the α-aminoalkylperoxyl moiety brings lower-energy pathways into play. In Figure 3, we notice that at around 20 kcal mol^{-1} below the entrance channel energy, the $NH_2CH(OO^{\bullet})CO_2^-$ radical can undergo an intramolecular hydrogen abstraction with concerted expulsion of CO_2, with the remaining ion then fragmenting to the $^{\bullet}OH$ radical and the formamide anion ^-NHCHO. This process has been identified as the dominant reaction pathway in the oxidation of peptidic α-carboxylate radical anions such as acetylglycinate ($CH_3C(O)$-$NH^{\bullet}CHCO_2^-$) due to the presence of the amide functionality.[18] The present results provide evidence for this mechanism as a minor reaction channel, which accounts for the m/z 44 product observed in Figure 2. While the ion abundance is too low for accurate determination of the branching ratio for this channel, an upper limit of 2% can be estimated, and thus, it is reasonable to ignore this pathway in the kinetic analysis, and we assume that m/z 72 is the exclusive reaction product from m/z 73.

The lowest-energy pathway in the α-aminoacetate radical anion reaction with O_2 is found to be for concerted H atom transfer and $HO_2{}^{\bullet}$ elimination via the transition-state structure depicted in Figure 4. This reaction proceeds with a barrier of only 8.6 kcal mol^{-1} (relative to the peroxyl radical), placing it

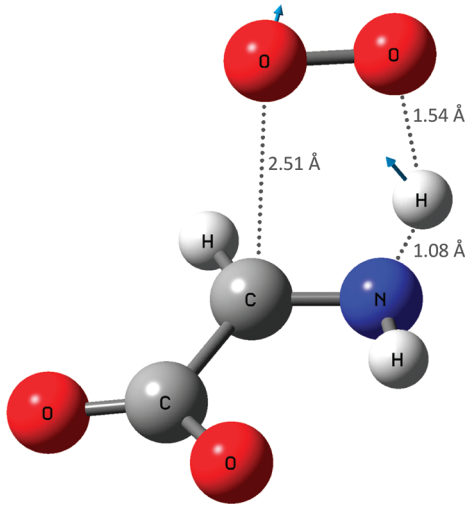

Figure 4. Transition-state structure for concerted $HO_2{}^{\bullet}$ elimination in the $NH_2CH(OO^{\bullet})CO_2^-$ radical anion at the B3LYP/6-31G(2df,p) level. Displacement vectors for the imaginary vibrational mode are illustrated.

27.7 kcal mol^{-1} below the entrance channel energy. This process produces a strongly hydrogen-bound complex (more stable than the isomeric peroxyl radical), which can dissociate to the imine $NHCHCO_2^-$ and the $HO_2{}^{\bullet}$ radical via a barrierless reaction, in a mechanism that is 19.9 kcal mol^{-1} exothermic overall. This very low energy reaction explains the major ionic reaction product observed at m/z 72 in the $NH_2{}^{\bullet}CHCO_2^-$ + O_2 reaction.

dx.doi.org/10.1021/jz300118k | J. Phys. Chem. Lett. 2012, 3, 805–811

So as to better understand the reaction kinetics, we have developed a master equation (ME) model of the $NH_2^{\bullet}CHCO_2^-$ + O_2 reaction system, based on the energy surface depicted in Figure 3. ME simulations indicate that the vibrationally excited peroxyl radical adduct has dissociated before the first bath gas collision at 307 K and 2.5 mTorr He. This is attributed to the abundance of negative-energy reaction channels and the low experimental pressure. Calculated rate constants and efficiencies for important reaction channels at the experimental conditions are included in Table 1, along with the corresponding experimental results, where we observe excellent agreement. The elimination of $HO_2^{\bullet}$ to form the m/z 72 product is predicted to account for 96.4% of the product yield, with the CO_2 + $^{\bullet}OH$ loss channel to m/z 44 responsible for 3.4% of the total reaction flux. The higher-energy carbonate radical anion channel, which could not be observed experimentally, yielded only 0.1% of the total products. Furthermore, the reverse reaction to $NH_2^{\bullet}CHCO_2^-$ + O_2 only accounted for 0.1% of the overall reaction flux, indicating a total reaction efficiency of 99.9%. Importantly, the close agreement between experiment and theory supports the proposed reaction mechanism (as well as validating the selected theoretical methods), confirming that $HO_2^{\bullet}$ elimination dominates in reactions of the $NH_2CH(OO^{\bullet})CO_2^-$ radical anion. Moreover, the simulations verify that this ion–molecule reaction does indeed proceed at essentially 100% reaction efficiency under the temperature and pressure conditions of the ion trap due to the very low barrier height for this α-aminoalkylperoxyl $HO_2^{\bullet}$ elimination process.

Table 1. Rate Constants (k) and Reaction Efficiencies[a] (ε) in the α-Aminoacetate Radical Anion ($NH_2C^{\bullet}HCO_2^-$) + O_2 Reaction, from Experiment and ME Simulations

	k (cm^3 molecule^{-1} s^{-1})		ε (%)	
	experiment[b]	ME	experiment	ME
$NH_2^{\bullet}CHCO_2^-$ + O_2 → $NHCHCO_2^-$ + $HO_2^{\bullet}$	6.4×10^{-10}	6.0×10^{-10}	100	96.4
$NH_2^{\bullet}CHCO_2^-$ + O_2 → ^-NHCHO + CO_2 + $^{\bullet}OH$	[c]	2.1×10^{-11}	[c]	3.4

[a]Defined as 100 × ($k/k_{collision}$). [b]Uncertainties in experimental rate constants and branching ratios are discussed in the Methods section. [c]The yield is too low to be accurately determined, but it is estimated to be <2% of the total products.

In order to explore if $HO_2^{\bullet}$ elimination is a general mechanism available to α-aminoalkylperoxyl radicals, we have constructed a theoretical energy surface for the archetypal α-aminomethyl radical ($NH_2CH_2^{\bullet}$) + O_2 reaction (Figure 5). Compared to its ionic counterpart (cf. Figure 3), the peroxyl radical is formed with slightly less energy (33 versus 36 kcal mol^{-1} exothermic), but the $HO_2^{\bullet}$ elimination barrier is similar, at around 10 kcal mol^{-1} above the peroxyl radical. For dissociation of the $NHCH_2\cdots HO_2^{\bullet}$ complex, the reaction enthalpy is 20 kcal mol^{-1} above the peroxyl radical, or about 13 kcal mol^{-1} below the entrance channel energy. Even at conditions commonly encountered in the troposphere (ca. 298 K and 1 atm) or in flames (>600 K and up to tens of atm), this reaction would be expected to proceed directly to the imine product + $HO_2^{\bullet}$. Further experimental and theoretical work is now required, however, to confirm that this process operates in the oxidation chemistry of neutral α-aminoalkyl radicals and to better characterize the kinetics. Note also that a direct abstraction transition state, with a small barrier height (0.9 kcal mol^{-1}), is also illustrated in Figure 5 (the corresponding structure could not be located for glycyl + O_2). This reaction will become important in combustion systems but will be slow relative to barrierless O_2 addition at room temperature and below.

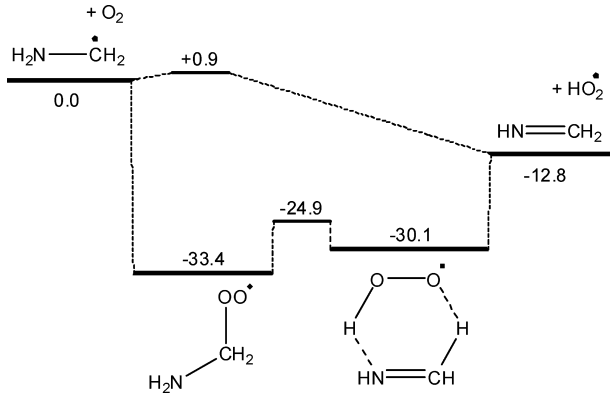

Figure 5. Ab initio energy surface for the α-aminomethyl radical + O_2 reaction. G3SX enthalpies for 0 K are shown in units of kcal mol^{-1}.

There is scant experimental data available for α-aminoalkyl radical + O_2 reactions. Masaki et al.[20] and la Cour Jansen et al.[21] did independently study the aminomethyl radical + O_2 reaction in the gas phase (298 K), measuring respective rate constants of 3.5×10^{-11} cm^3 molecule^{-1} s^{-1} at 0.6–6 Torr of N_2[20] and 8.1×10^{-11} cm^3 molecule^{-1} s^{-1} at 760 Torr of SF_6.[21] This is consistent with a rapid neutral–neutral recombination reaction proceeding at close to the collision limit, but the lack of product detection provides little information about the mechanism. Moreover, it is unclear if the rate constant differences arise from a pressure effect (indicating collisional deactivation of the peroxyl radical) or from experimental uncertainty. Just prior to the work of Masaki et al., Schade and Crutzen[7] considered the atmospheric chemistry of amine emissions from animal husbandry and proposed a mechanism by which the aminomethyl radical reacts with O_2 to form the peroxyl radical and the imine $NH{=}CH_2$ + $HO_2^{\bullet}$. In a prescient observation, they suggested that the direct $HO_2^{\bullet}$ elimination pathway would dominate, from analogy with the hydroxymethyl radical. It was also proposed that further photochemical processing of $NH{=}CH_2$ would lead to N_2O, HCN, and NH_3 production, whereas the peroxyl radical (if it could indeed be formed) would be expected to yield formamide.

The facile elimination of $HO_2^{\bullet}$ from α-aminoalkyl radicals was first observed experimentally in our recent study of peptidic α-carboxylate radical oxidation, where it appeared as a minor reaction channel.[18] The present study reveals, however, that this novel process can dominate in the reaction chemistry of simple α-aminoalkylperoxyl radicals. Although this appears to be a new mechanism, the elimination of $HO_2^{\bullet}$ from other α-substituted peroxyl radicals is relatively well-known. In the prototypical ethylperoxyl radical ($CH_3CH_2OO^{\bullet}$), the concerted elimination process to $CH_2{=}CH_2$ + $HO_2^{\bullet}$ is now well-established from both theory and experiment, although uncertainties with respect to the reaction energetics and mechanism certainly remain.[3,22] This process, which can be extended to other n-alkyl radical + O_2 reactions, requires a relatively large barrier (on the order of 30 kcal mol^{-1}), which typically places it just below the alkyl radical + O_2 energy.

dx.doi.org/10.1021/jz300118k | J. Phys. Chem. Lett. 2012, 3, 805–811

When the α-alkyl substituent in this mechanism is replaced by a hydroxyl group, however, the concerted $HO_2^\bullet$ elimination mechanism is retained, although now the barrier is reduced to well below the entrance channel energy.[23,24] At temperatures and pressures relevant to combustion and Earth's atmosphere, this results in a direct (chemically activated) reaction from an α-hydroxyalkyl radical + O_2 to an aldehyde + $HO_2^\bullet$, which has a particularly profound effect on the ignition behavior of alcohol fuels.[24] The concerted $HO_2^\bullet$ elimination mechanism observed here for α-aminoalkylperoxyl radicals extends this reaction series further and suggests that it may be a general mechanism for substituted peroxyl radicals (indeed, there is some theoretical evidence for a similar reaction taking place in the α-thiomethylperoxyl radical $HSCH_2OO^\bullet$).[25] Furthermore, this work implies that the $HO_2^\bullet$ radical can initiate imine oxidation through barrierless peroxyl radical formation in the same way that $HO_2^\bullet$ + alkene[26] and $HO_2^\bullet$ + carbonyl[27] reactions can.

The α-aminoalkyl radical oxidation mechanism revealed in this study will play an important role in the photochemical oxidation of primary and secondary amines. Abstraction of a H atom from the labile α-site in alkylamines will produce an α-aminoalkyl radical that is then expected to react with O_2 to directly form an imine + $HO_2^\bullet$. Because this mechanism completely bypasses the collisionally deactivated peroxyl radical, there is no opportunity for $RO_2^\bullet$ + $^\bullet NO \rightarrow RO^\bullet$ + $^\bullet NO_2$ reactions, which typically dominate in atmospheric peroxyl radical chemistry (particularly in urban environments). The conversion of $^\bullet NO$ to $^\bullet NO_2$ by peroxyl radicals, followed by photolysis to $^\bullet NO$ + $O(^3P)$ and subsequent association of the oxygen atom with O_2, is the major contributor to ground-level ozone in urban plumes. Reaction of $HO_2^\bullet$ with $^\bullet NO$ and O_3, however, also represents a major $^\bullet OH$ radical source, which helps to maintain oxidative capacities in polluted air masses characterized by high levels of NO_x and volatile organics. The impact that high amine fluxes to the troposphere from amine CCS plants, as well as amine structure (primary/secondary versus tertiary), ultimately have on urban air quality and oxidative capacities remains to be seen, although the chemistry identified here is sure to be involved.

METHODS

Mass Spectrometry. A 10−50 μM methanolic solution of glutamic acid, raised to high pH with aqueous ammonia, was infused at a rate of 3−5 μL/min into the electrospray ionization source of a ThermoFisher (San Jose, CA) LTQ linear quadrupole ion trap mass spectrometer. Methanol (HPLC grade) and ammonia solution (28%) were obtained from Ajax Finechem (Sydney, Australia). Glutamic acid was obtained from Stansen Scientific (Adelaide, Australia). Modifications to the mass spectrometer to perform both photodissociation and ion−molecule reactions in the trap have been described elsewhere.[17,18] Briefly, a 2.75 in. quartz viewport (MDC Vacuum Products, Hayward, CA) is fitted on the posterior plate of the vacuum manifold with a CF flange to allow transmission of the 266 nm laser pulse (~2.4 mJ/pulse) from a Nd:YAG laser (Continuum, Santa Clara, CA). Ion−molecule reactions may be conducted by introducing a flow of neutral reagent via a syringe pump into a flow of ultra-high-purity (UHP) helium (3−5 psi) through a heated septum input (25−250 °C). The gas mixture was introduced into the ion trap via a variable leak valve, which was adjusted to afford an ion trap pressure of ~2.5 mTorr. The temperature of the ion trap was measured at 307 ± 1 K, which was taken as the effective temperature of the ion−molecule reactions observed within.[12] Reaction times of 30−1000 ms were set using the excitation time parameter within the XCalibur control software (Thermo-Fisher, San Jose, CA) using a fragmentation energy of 0 (arbitrary units). All spectra represent an average of at least 50 scans. The concentration of dioxygen in the ion trap was measured using a calibrant reaction, where the second-order rate constant is known (3-carboxylatoadamantyl radical anion + O_2); thus, the $[O_2]$ is simply $k_{pseudofirst}/k_{second}$. Rate constants were obtained from the least-squares fit to the pseudo-first-order decay profiles, with all measurements repeated six times, and are reported in the text with one standard deviation comprising the statistical uncertainty. Rate constants measured using this experimental configuration are assigned at ±25% to account for statistical and systematic uncertainties.[17] Collision rate constants $k_{collision}$ for the ion−molecule reactions were estimated by the parametrized trajectory theory of Su and Chesnavich,[28] which, for the radical anion + dioxygen reaction, reduces to the Langevin theory result. Collision rate constants allow for the calculation of reaction efficiencies ε [%] as $\varepsilon = 100 \times (k/k_{collision})$.

Theory. The composite G3SX method[29] has been used to characterize stationary points in the $NH_2^\bullet CHCO_2^-$ + O_2 and $NH_2CH_2^\bullet$ + O_2 reaction mechanisms. For ambiguous transition-state structures, intrinsic reaction coordinate (IRC) scans were used to confirm reactant and product identities. The G3SX method was chosen as it demonstrates excellent performance for barrier heights and reaction energies relative to computational cost, and quoted energies are expected to be accurate to within 1 kcal mol^{-1}, on average.[29,30] All calculations were performed using Gaussian 09.[31] Theoretical rate constants in the $NH_2^\bullet CHCO_2^-$ + O_2 reaction system were obtained from a ME model developed in MultiWell-2011.3.[32−35] Micro-canonical rate constants were from RRKM theory, based on moments of inertia and vibrational frequencies calculated at the B3LYP/6-31G(2df,p) level of theory. Internal degrees of freedom were treated as harmonic oscillators, with external degrees of freedom described using an active 1D and an inactive 2D rotor, assuming symmetric tops. Collisional energy transfer between He and the isomeric $C_2NO_4H_3^-$ wells is described using the common single exponential-down model, with a small value of ΔE_{down} (100 cm^{-1})[36] and Lennard-Jones parameters of 6.0 Å and 350 K. The energy-grained component of Barker's hybrid ME formulation was solved for energies up to 30 000 cm^{-1} with a grain size of 10 cm^{-1}, with the continuum component then carried on to 200 000 cm^{-1}. Tunnelling is incorporated for H-shift reactions using an Eckart barrier (this includes the concerted H-shift/$HO_2^\bullet$ elimination, where C−O bond cleavage is early and H-atom transfer dominates in the vicinity of the transition state). Transition states for barrierless reactions were modeled using the hindered Gorin approach,[37] with rate constants set to the parametrized trajectory theory collision rates. ME simulations were performed at the ion trap conditions of 307 K and 2.5 mTorr of He, and ten million trials were conducted so as to obtain accurate statistics for low-yielding channels.

ASSOCIATED CONTENT

Supporting Information

Mass spectrum and reaction scheme for ^{13}C-labeled glutamic acid. Pseudo-first-order rate plot for the α-aminoacetate radical anion + O_2 reaction. Mass spectra illustrating the effect of O_2 concentration on depletion of the α-aminoacetate radical anion

dx.doi.org/10.1021/jz300118k | J. Phys. Chem. Lett. 2012, 3, 805−811

(m/z 73) with the concomitant formation of the m/z 72 product. Optimized structures, vibrational frequencies, and moments of inertia for wells and transition states in the ME model. This material is available free of charge via the Internet at http://pubs.acs.org.

AUTHOR INFORMATION

Corresponding Author

*E-mail. gdasilva@unimelb.edu.au (G.d.S.); blanksby@uow.edu.au (S.J.B.).

Notes

The authors declare no competing financial interest.

ACKNOWLEDGMENTS

We are grateful to the Australian Research Council (ARC) for funding through the Discovery Projects scheme (DP1094135 [A.J.T.]; DP110103889 [G.d.S.]) and the ARC Centre of Excellence in Free Radical Chemistry and Biotechnology (CE0561607 [S.J.B.]). Computational resources provided in part by the Victorian Partnership for Advanced Computing (VPAC).

REFERENCES

(1) Halliwell, B.; Gutteridge, J. M. C. *Free radicals in biology and medicine*, 3rd ed.; OUP: Oxford, U.K., 1999.

(2) Lightfoot, P. D.; Cox, R. A.; Crowley, J. N.; Destriau, M.; Hayman, G. D.; Jenkin, M. E.; Moortgat, G. K.; Zabel, F. Organic Peroxy Radicals: Kinetics, Spectroscopy and Tropospheric Chemistry. *Atmos. Environ.* **1992**, *26A*, 1805−1961.

(3) Zador, J.; Taatjes, C. A.; Fernandes, R. X. Kinetics of Elementary Reactions in Low-Temperature Autoignition Chemistry. *Prog. Energy Combust. Sci.* **2011**, *37*, 371−421.

(4) Stadtman, E. R.; Levine, R. L. Free Radical-Mediated Oxidation of Free Amino Acids and Amino Acid Residues in Proteins. *Amino Acids* **2003**, *25*, 207−218.

(5) Miller, J. A.; Bowman, C. T. Mechanism and Modeling of Nitrogen Chemistry in Combustion. *Prog. Energy Combust. Sci.* **1989**, *15*, 287−338.

(6) Dean, A. M.; Bozzelli, J. W. Combustion Chemistry of Nitrogen. In *Gas-Phase Combustion Chemistry*; Gardiner, W. C., Ed.; Springer: New York, 1999.

(7) Schade, G. W.; Crutzen, P. J. Emission of Aliphatic Amines from Animal Husbandry and their Reactions: Potential Source of N_2O and HCN. *J. Atmos. Chem.* **1995**, *22*, 319−346.

(8) Rochelle, G. T. Amine Scrubbing for CO_2 Capture. *Science* **2009**, *325*, 1652−1654.

(9) Nielsen, C. J.; et al. Atmospheric Chemistry of 2-Aminoethanol (MEA). *Energy Procedia* **2011**, *4*, 2245−2252.

(10) Kenttämaa, H. Ion−Molecule Reactions of Distonic Radical Cations. In *Encyclopedia of Mass Spectrometry*; Nibbering, N. M. M., Ed.; Elsevier: Amsterdam, The Netherlands, 2005.

(11) Petzold, C. J.; Nelson, E. D.; Lardin, H. A.; Kenttämaa, H. I. Charge-Site Effects on the Radical Reactivity of Distonic Ions. *J. Phys. Chem. A* **2002**, *106*, 9767−9775.

(12) Yu, D.; Rauk, A.; Armstrong, D. A. Radicals and Ions of Glycine: An ab Initio Study of the Structures and Gas-Phase Chemistry. *J. Am. Chem. Soc.* **1995**, *117*, 1789−1796.

(13) Bonifacic, M.; Stefanic, I.; Hug, G. L.; Armstrong, D. A.; Asmus, K.-D. Glycine Decarboxylation: The Free Radical Mechanism. *J. Am. Chem. Soc.* **1998**, *120*, 9930−9940.

(14) Nicolet, Y.; Martin, L.; Tron, C.; Fontecilla-Camps, J. C. A Glycyl Free Radical as the Precursor in the Synthesis of Carbon Monoxide and Cyanide by the [FeFe]-Hydrogenase Maturase HydG. *FEBS Lett.* **2010**, *584*, 4197−4202.

(15) Hug, G. L.; Fessenden, R. W. Identification of Radicals and Determination of Their Yields in the Radiolytic Oxidation of Glycine. Time-Resolved ESR Methodology. *J. Phys. Chem. A* **2000**, *104*, 7021−7029.

(16) Stefanic, I.; Ljubic, I.; Bonifacic, M.; Sabljic, A.; Asmus, K.-D.; Armstrong, D. A. A Surprisingly Complex Aqueous Chemistry of the Simplest Amino Acid. A Pulse Radiolysis and theoretical Study on H/D Kinetic Isotope Effects in the Reaction of Glycine anions with Hydroxyl Radicals. *Phys. Chem. Chem. Phys.* **2009**, *11*, 2256−2267.

(17) Harman, D. G.; Blanksby, S. J. Investigation of the Gas Phase Reactivity of the 1-Adamantyl Radical Using a Distonic Radical Anion Approach. *Org. Biomol. Chem.* **2007**, *5*, 3495−3503.

(18) Ly, T.; Kirk, B. B.; Hettiarachchi, P. I.; Poad, B. L. J.; Trevitt, A. J.; da Silva, G.; Blanksby, S. J. Reactions of Simple and Peptidic Alpha-Carboxylate Radical Anions with dioxygen in the Gas Phase. *Phys. Chem. Chem. Phys.* **2011**, *13*, 16314−16323.

(19) Kirk, B. B.; Harman, D. G.; Blanksby, S. J. Direct Observation of the Gas Phase Reaction of the Cyclohexyl Radical with Dioxygen Using a Distonic Radical Ion Approach. *J. Phys. Chem. A* **2010**, *114*, 1446−1456.

(20) Masaki, A.; Tsunashima, S.; Washida, N. Rate Constants for Reactions of Substituted Methyl Radicals (CH_2OCH_3, CH_2NH2, CH_2I, and CH_2CN) with O_2. *J. Phys. Chem.* **1995**, *99*, 13126−13131.

(21) la Cour Jansen, T.; Trabjerg, I.; Rettrup, S.; Pagsberg, P.; Silesen, A. Experimental and Theoretical Investigation of the UV Spectrum and Kinetics of the Aminomethyl Radical, CH_2NH_2. *Acta Chem. Scand.* **1999**, *53*, 1054−1058.

(22) Wilke, J. J.; Allen, W. D.; Schaefer, H. F. III. Establishment of the $C_2H_5 + O_2$ Reaction Mechanism: A Combustion Archetype. *J. Chem. Phys.* **2008**, *128*, 174308.

(23) Zador, J.; Fernandes, R. X.; Georgievskii, Y.; Meloni, G.; Taatjes, C. A.; Miller, J. A. The Reaction of Hydroxyethyl Radicals with O_2: A Theoretical Analysis and Experimental Product Study. *Proc. Combust. Inst.* **2009**, *32*, 271−277.

(24) da Silva, G.; Bozzelli, J. W.; Liang, L.; Farrell, J. T. Ethanol Oxidation: Kinetics of the α-Hydroxyethyl Radical + O_2 Reaction. *J. Phys. Chem. A* **2009**, *113*, 8923−8933.

(25) Tang, Y.-Z.; Pan, Y.-R.; Sun, J.-Y.; Sun, H.; Wang, R.-S. DFT and ab Initio Study on the Reaction Mechanism of $CH_2SH + O_2$. *Theor. Chem. Acc.* **2008**, *121*, 201−207.

(26) Zador, J.; Klippenstein, S. J.; Miller, J. A. Pressure-Dependent OH Yields in Alkene + HO_2 Reactions: A Theoretical Study. *J. Phys. Chem. A* **2011**, *115*, 10218−10225.

(27) da Silva, G.; Bozzelli, J. W. Role of the α-Hydroxyethylperox Radical in the Reactions of Acetaldehyde and Vinyl Alcohol with HO_2. *Chem. Phys. Lett.* **2009**, *483*, 25−29.

(28) Su, T.; Chesnavich, W. J. Parameterization of the Ion−Polar Molecule Collision Rate Constant by Trajectory Calculations. *J. Chem. Phys.* **1982**, *76*, 5183−5185.

(29) Curtiss, L A.; Redfern, P. C.; Raghavachari, K.; Pople, J. A. Gaussian-3X (G3X) Theory: Use of Improved Geometries, Zero-Point Energies and Hartree−Fock Basis Sets. *J. Chem. Phys.* **2001**, *114*, 108.

(30) Zheng, J.; Zhao, Y.; Truhlar, D. G. The DBH24/08 Database and Its Use to Assess Electronic Structure Model Chemistries for Chemical Reaction Barrier Heights. *J. Chem. Theory Comput.* **2009**, *5*, 808−821.

(31) Frisch, M. J.; Trucks, G. W.; Schlegel, H. B.; Scuseria, G. E.; Robb, M. A.; Cheeseman, J. R.; Scalmani, G.; Barone, V.; Mennucci, B.; Petersson, G. A. et al. *Gaussian 09*, revision B.01; Gaussian, Inc.: Wallingford, CT, 2010.

(32) *MultiWell-2011.3 Software*. Designed and maintained by John R. Barker with contributors Nicholas F. Ortiz, Jack M. Preses, Lawrence L. Lohr, Andrea Maranzana, Philip J. Stimac, T. Lam Nguyen, and T. J. Dhilip Kumar; University of Michigan, Ann Arbor, MI; http://aoss.engin.umich.edu/multiwell/ (2011).

(33) Barker, J. R. Multiple-Well, Multiple-Path Unimolecular Reaction Systems. I. MultiWell Computer Program Suite. *Int. J. Chem. Kinet.* **2001**, *33*, 232−245.

(34) Barker, J. R. Energy Transfer in Master Equation Simulations. *Int. J. Chem. Kinet.* **2009**, *41*, 748−763.

(35) Nguyen, T. L.; Barker, J. R. Sums and Densities of fully Coupled Anharmonic Vibrational States: A Comparison of three Practical Approaches. *J. Phys. Chem. A* **2010**, *114*, 3718−3730.
(36) Lam, A. K. Y.; Li, C.; Khairallah, G.; Kirk, B. B.; Blanksby, S. J.; Trevitt, A. J.; Wille, U.; O'Hair, R. A. J.; da Silva, G. Gas-Phase Reactions of Aryl Radicals with 2-Butyne: Experimental and Theoretical Investigation Employing the *N*-Methyl-pyridinium-4-yl Radical Cation. *Phys. Chem. Chem. Phys.* **2012**, *14*, 2417−2426.
(37) Smith, G. P.; Golden, D. M. Application of RRKM Theory to the Reactions OH + NO_2 + N_2 → $HONO_2$ + N_2 (1) and ClO + NO_2 + N_2 → $ClONO_2$ + N_2 (2); A Modified Gorin Model Transition State. *Int. J. Chem. Kinet.* **1978**, *10*, 489−501.